JOURNAL OF MAGNETIC RESONANCE 87, 620–627 (1990)

Practical Aspects of Proton–Carbon–Carbon–Proton Three-Dimensional Correlation Spectroscopy of ^{13}C-Labeled Proteins

AD BAX, G. MARIUS CLORE, PAUL C. DRISCOLL, ANGELA M. GRONENBORN, MITSUHIKO IKURA, AND LEWIS E. KAY

Laboratory of Chemical Physics, NIDDK, National Institutes of Health, Bethesda, Maryland 20892

Received January 4, 1990

The determination of protein solution structures by NMR requires complete assignment of both the backbone and the amino acid side-chain resonances. For larger proteins, such assignments can be difficult to obtain because of extensive resonance overlap in the 2D ^{1}H–^{1}H correlation spectra. The overlap problem can be substantially reduced by separating homonuclear correlation spectra in a three-dimensional experiment, combining the homonuclear correlation techniques with a heteronuclear multiple-quantum correlation (HMQC) experiment. Such 3D NOESY-HMQC and HOHAHA-HMQC techniques work well for ^{15}N-labeled proteins (*1–3*). Very recently, it has been demonstrated that the 3D NOESY-HMQC technique can also be used for ^{13}C-labeled proteins (*4, 5*). However, separating homonuclear *J*-correlation spectra according to the chemical-shift frequencies of attached ^{13}C nuclei, as previously used for smaller molecules (*6, 7*), is inefficient for macromolecules. The main reason for this stems from the severe heteronuclear dipolar line broadening of the protons attached to ^{13}C, making the J_{HH} transfer very inefficient.

Recently, we proposed a new three-dimensional NMR experiment, known as HCCH, in which magnetization is transferred between vicinal protons in a three-step manner (*8*). In the first step, ^{1}H magnetization is transferred to its attached ^{13}C nucleus via the large and well-resolved $^1J_{CH}$ coupling ($\sim$140 Hz). In the second step, ^{13}C magnetization is transferred to its ^{13}C neighbor(s) via the relatively large $^1J_{CC}$ coupling (33–45 Hz). Finally ^{13}C magnetization is transferred back to ^{1}H via the $^1J_{CH}$ coupling. To maximize sensitivity, this HCCH experiment requires a high level (>90%) of uniform ^{13}C labeling.

Since magnetization is transferred through one-bond couplings that to first order are independent of dihedral angles, the transfer efficiency is independent of local geometry, in contrast to conventional homonuclear correlation methods. Because all three individual transfer steps are highly effective, the HCCH experiment transfers a substantial fraction of magnetization from one proton to its vicinal partners, despite the relatively large ^{1}H linewidth.

Although spectra previously obtained with the HCCH method show many of the desired correlations, they were plagued by relatively high levels of t_1 noise and spectral artifacts (*8*). In the present Communication we address the sources of these undesirable features and demonstrate improvements that greatly reduce their intensity.

0022-2364/90 $3.00

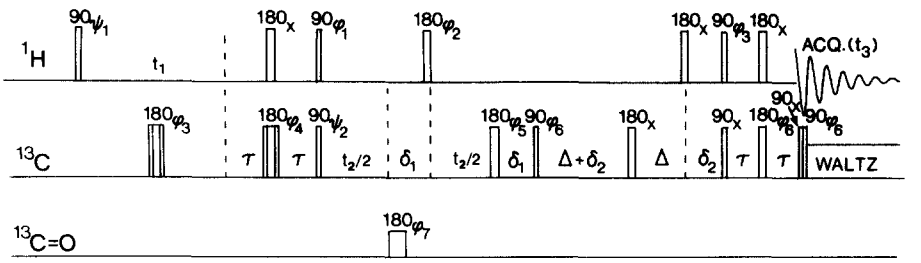

FIG. 1. Pulse sequence of the HCCH 3D experiment. For adequate suppression of artifacts, the sequence requires a 16-step phase cycle: $\phi_1 = y, -y$; $\phi_2 = 4(x), 4(y), 4(-x), 4(-y)$; $\phi_3 = 8(x), 8(-x)$; $\phi_4 = 2(x), 2(-x)$; $\phi_5 = 2(x), 2(y), 2(-x), 2(-y)$; $\phi_6 = 4(x), 4(-x)$; $\phi_7 = 8(x), 8(y)$; Acq. $= 2(x, -x, -x, x), 2(-x, x, x, -x)$. The ^{13}C carrier is positioned in the center of the aliphatic region and the $180^\circ_{\phi 7}$ carbonyl pulse is generated by means of a DANTE sequence. The $180^\circ_{\phi 3}$ and $180^\circ_{\phi 4}$ pulses are of the composite type $(90^\circ_x 180^\circ_y 90^\circ_x)$. Quadrature in the F_1 and F_2 dimensions is obtained with the TPPI–States method (*19*), using $\psi_1 = 16(x), 16(y)$; $\psi_2 = 32(x), 32(y)$. Each time t_1 is incremented, the receiver reference phase and ψ_1 are also incremented by 180°. Each time t_2 is incremented the receiver phase and ψ_2 are also incremented by 180°. Data obtained for $\psi_1 = x, y$ and $\psi_2 = x, y$ are stored separately and processed as complex data.

Figure 1 illustrates the improved HCCH pulse sequence. For the simple case of two coupled carbons, C_A and C_B with attached protons H_A and H_B, magnetization is transferred from H_A to H_B as follows. At the end of the ^{1}H evolution period, t_1, proton magnetization (H_A) is transferred to ^{13}C (C_A) in an INEPT-like manner (*9, 10*). The C_A transverse magnetization which is antiphase with respect to the polarization of H_A becomes in-phase during the two delays, δ_1, and proton decoupling during the t_2 evolution period is accomplished by the 180° ^{1}H pulse applied at the center of t_2. During t_2 (as well as the delays δ_1), C_A magnetization becomes antiphase with respect to its ^{13}C coupling partner, C_B, at a rate that is determined by $^1J_{CC}$. The $90^\circ_{\phi 6}$ pulse subsequently transfers this antiphase C_A magnetization into antiphase C_B magnetization in a COSY-type manner. During the following interval, $2\Delta + 2\delta_2$, the antiphase C_B magnetization becomes in-phase with respect to C_A, and the 180° ^{1}H pulse (applied at time δ_2 before the final set of simultaneous 90° pulses) ensures that the refocused C_B magnetization is antiphase with respect to its attached proton, H_B. The final sets of 90° and 180° pulses then constitute a reverse refocused INEPT, transferring C_B magnetization to H_B.

During repeated use of our original pulse scheme (*8*), we found two separate problems that cause artifacts and noise-like features in the 3D spectra. It is well known that artifacts generally result from undesired coherence transfer pathways and, as will be discussed later, can be largely removed by extensive phase cycling. The noise-like features were found to originate from modulation sidebands of the composite pulse decoupling cycle used. As pointed out previously (*11*), these modulation sidebands average to zero if the decoupling is executed in an asynchronous manner and many transients are coadded. Because of the large number of t_1 and t_2 increments required for a 3D experiment, the number of transients per pair of (t_1, t_2) values is limited in practice to about 16 because of measuring time constraints. Consequently, averaging of the modulation sidebands is incomplete. The approach we have taken minimizes the amount of composite pulse decoupling in the sequence of Fig. 1, by using 180° pulses at the midpoints of the t_1 and t_2 intervals to remove the net effect of the unde-

sired couplings. However, during the detection period, t_3, composite pulse decoupling is essential. As will be described in more detail elsewhere, the intensity of modulation sidebands originating from incompletely refocused ^{1}H magnetization (I_yS_z type terms) can be reduced by inserting a 90°_x–$90^\circ_{\pm x}$ ^{13}C pulse pair prior to the start of the decoupling, as indicated in Fig. 1. This pulse pair has the effect of inverting S_z on alternate scans, canceling signals originating from I_yS_z.

In order to maximize magnetization transfer between the Cα and Cβ carbons, it is important to remove the effects of Cα–carbonyl coupling during the delays $t_2 + 2\delta_1$ and $2\Delta + 2\delta_2$. For the delay $2\Delta + 2\delta_2$, this is accomplished by ensuring that the 180°_x pulse causes minimal excitation of the carbonyls. Since the carbonyl resonances are centered at about 177 ppm, whereas the carrier is positioned in the center of the aliphatic region, at 43 ppm, the power and duration of the 180°_x pulse must be adjusted such that this pulse has a null in its excitation profile at the carbonyl frequency. During the t_2 period, decoupling is achieved by a 180° pulse applied to the carbonyls. This pulse should be applied in such a way that aliphatic resonances are only minimally affected. Ideally, a shaped selective inversion pulse is used for this purpose. Due to hardware limitations, however, we were forced to use a less ideal but still adequate solution, applying a rectangular carbonyl inversion pulse with low RF power (180° pulse width ~400 μs). This carbonyl inversion pulse can be made phase coherent with the other ^{13}C pulses (avoiding randomness of any spurious excitation of aliphatic resonances) by generating it as a DANTE-type pulse (*12, 13*). Thus, the carbonyl inversion pulse was applied as eight repetitions of the cycle (4°_0, 4°_{-300}, 4°_{-240}, 4°_{180}, 4°_{120}, 4°_{60}), where the RF power level is adjusted such that the duration of an individual cycle equals $1/\delta$, where δ is the offset of the carbonyl resonances from the RF carrier. Long-range couplings between carbonyls and protons are small relative to the ^{1}H linewidth, and carbonyl decoupling during the t_1 and t_3 periods is therefore not necessary.

The large variety of relatively weak artifacts found in 3D spectra recorded with our original pulse sequence (*8*) prompted us to reconsider the phase-cycling scheme used, in order to ensure that only the desired coherence transfer pathway (*14*) would give rise to magnetization detected during t_3. In designing a good phase-cycling scheme, a difficult constraint is imposed by the fact that available measuring time limits the number of scans per (t_1, t_2) pair to at most 16, thus restricting the number of phase-cycling steps.

A single undesired coherence transfer pathway can usually be eliminated by a simple two-step phase cycle. For example, phase inversion of all preparation period pulses in a 2D experiment suppresses axial peaks. If a second source of artifacts must be suppressed additional phase cycling is required. For example, in the case of a NOESY experiment single-quantum coherent transfer can be suppressed by phase alternation of the last pulse. If both types of phase cycling were executed simultaneously (resulting in a two-step cycle), single-quantum coherent transfer of axial signals would not be suppressed in the final spectrum. For this reason, phase-cycling steps are usually executed in an independent manner. For the case of the NOESY experiment, combination of two 2-step phase cycles results in a $2 \times 2 = 4$-step phase cycle.

Because of the large number of possible spurious transfer pathways combined with the limited number of available scans per (t_1, t_2) pair in our present 3D experiment, we were forced to consolidate several of the phase-cycling steps. Two phase cycles may, in general, be executed simultaneously if their purpose is to eliminate two unrelated sources of artifacts. In such a case, if the first phase cycle completely cancels undesired magnetization that would result in an artifact with fractional intensity, a, and the second phase cycle cancels a second type of artifact of fractional intensity, b, executing the two phase cycles simultaneously will leave residual artifacts with very low fractional intensity, $a \times b$, in the final spectrum.

Using this type of reasoning, supplemented by the experimental results of several dozen trial phase cycles, we developed the 16-step phase cycle given in the legend to Fig. 1, which affords near-optimal suppression of artifacts. In addition, the first two 180° ^{13}C pulses were of the composite type ($90^\circ_x 180^\circ_y 90^\circ_x$) to compensate for offset and RF inhomogeneity effects (*15*).

The effectiveness of the pulse sequence of Fig. 1 is demonstrated for a 1.8 mM sample of the protein interleukin-1β (156 residues, 17 kDa), dissolved in D_2O, p^{2}H 5.2, 35°C. Spectra were recorded on a Bruker AM-600 spectrometer that had been modified to eliminate overhead time at the end of every t_1 and t_2 increment. The ^{1}H carrier was positioned at 3.0 ppm, and the ^{13}C carrier at 43 ppm. All proton pulses were applied with a 16 kHz RF field. ^{13}C pulses were applied using a 10 kHz RF field (~30 W RF power), and the DANTE-type carbonyl inversion pulse was applied with a weak 1.3 kHz RF field. For ^{13}C decoupling during data acquisition, the ^{13}C power was reduced to 3 W. Acquisition times were 28, 10, and 47 ms in the t_1, t_2, and t_3 dimension, respectively. The size of the acquired 3D matrix was (128 complex) × (32 complex) × (512 real). Using a delay time of 0.9 s between scans, the total measuring time was 70 h. 3D data were processed with a combination of commercial software (NMRI, Syracuse, New York) and home-written programs for Fourier transformation in the third dimension (*13*). In all three dimensions, 50°-phase-shifted sine-bell filtering and zero filling were used. For convenience, adjustment of delay durations was used to ensure that zero phase correction was required in both the F_1 and the F_2 dimensions of the final 3D spectrum. Thus, by adding the duration of the composite 180° ^{13}C pulse (100 μs) to the τ delay between the 180°_x and $90^\circ_{\phi 1}$ ^{1}H pulses, the required phase correction in the F_1 dimension becomes zero, independent of the ^{1}H pulse width. In the t_2 dimension, the $180^\circ_{\phi 2}$ ^{1}H pulse is applied at the end of the first δ_1 interval, eliminating the need for phase correction in the F_2 dimension.

In the t_2 dimension, magnetization transfer between J-coupled carbons has a $\sin \pi J_A(t_2 + 2\delta_1)\cos^n \pi J_P(t_2 + 2\delta_1)$ dependence, where J_A and J_P are the active and passive carbon–carbon coupling constants, $^1J_{CC}$, and n is the number of passive carbons. The sum of $2\delta_1$ plus the t_2 acquisition time is set to about $1/(2J_{CC})$ and, hence, the t_2 time-domain signal that contributes to the ^{1}H–^{1}H cross-peak intensity has an envelope shape similar to a sine bell, shifted by $2\delta_1$. Thus, the lineshape of a ^{1}H–^{1}H cross peak in the F_2 dimension is not Lorentzian, and in the absence of digital filtering looks similar to that of a singlet for which resolution enhancement with a shifted sine bell is used. The t_2 time-domain signal of the diagonal ($F_1 = F_3$) resonances has a $\cos \pi J_A(t_2 + 2\delta_1)\cos^n \pi J_P(t_2 + 2\delta_1)$ dependence, corresponding to a rapidly de-

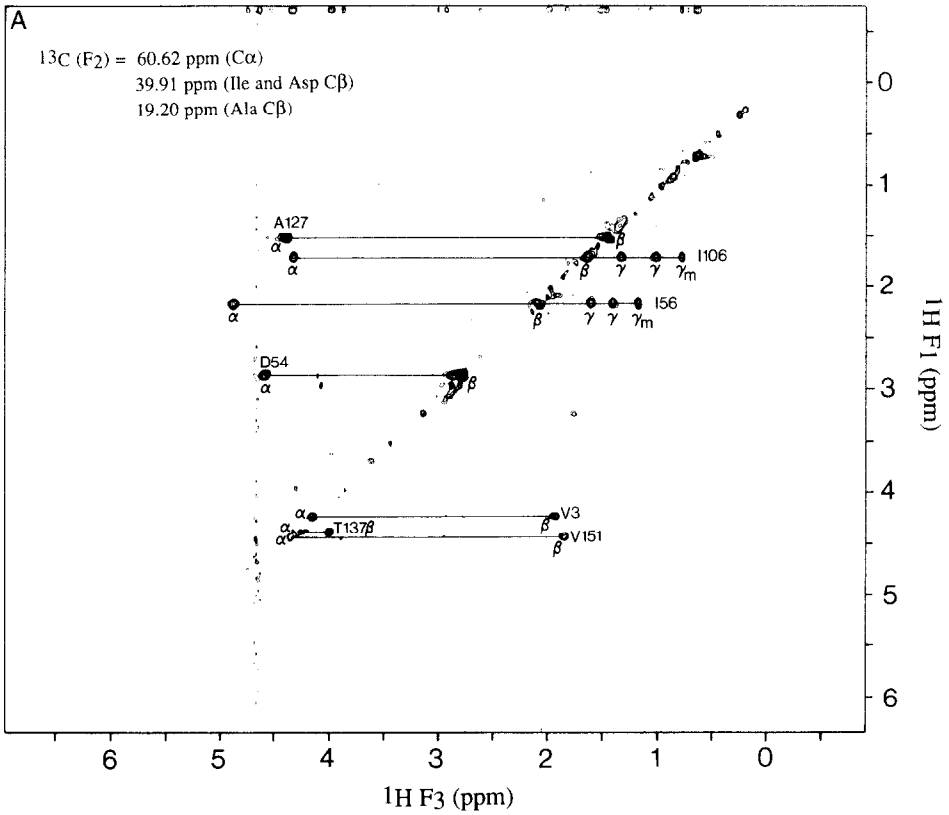

FIG. 2. F_1, F_3 slices of the 3D HCCH spectrum of interleukin-1β, recorded at 600 MHz. Because of extensive folding utilized in the F_2 dimension, each slice corresponds to three ^{13}C chemical shifts, indicated in each panel. Separation between slices in the F_2 dimension is 0.32 ppm (48 Hz). Diagonal resonances correspond to one-bond correlations between ^{13}C (F_2) and ^1H ($F_1 = F_3$) chemical shifts; cross peaks originate from magnetization transfer to protons that are geminal or vicinal with respect to the protons on the diagonal.

caying envelope shape, resulting in a broader F_2 linewidth than is observed for the cross peaks.

Figure 2 shows two (F_1, F_3) slices of the 3D spectrum of interleukin-1β. Assignment of the side-chain resonances in such slices is relatively straightforward once full sequence-specific assignments of the Cα carbons and Hα protons are available. Note that the Cα assignments for a protein the size of interleukin-1β usually cannot be obtained from a simple 2D ^1H–^{13}C correlation spectrum alone, because of the substantial degree of overlap in the Hα region of the spectrum. In the present case, Cα resonance assignments relied heavily on the use of a triple-resonance 3D experiment that correlates the backbone NH proton and ^{15}N chemical shifts with those of the intraresidue Cα carbon (*16*). Complete assignments of the backbone proton and ^{15}N resonances were obtained previously by using 3D NOESY-HMQC and NOESY-HOHAHA experiments (*17*).

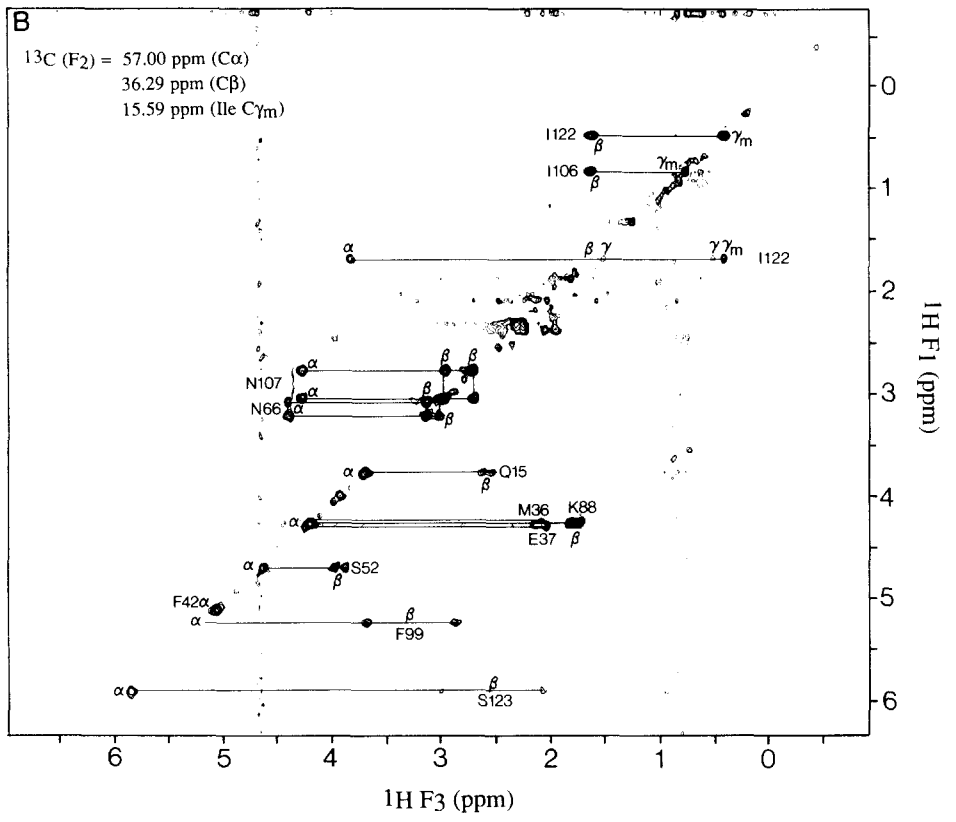

FIG. 2—*Continued*

The F_2 spectral width was set to only 20.7 ppm, resulting in extensive folding in the ^{13}C dimension. This folding affords a substantial increase in the F_2 resolution, without introducing any serious ambiguities. Even though each of the slices shown in Fig. 2 has three possible ^{13}C shift values associated with it, in all but very rare cases the F_3 coordinates of the diagonal and cross peaks allow identification of the ^{13}C shift value that corresponds to the diagonal peak. For example, in Fig. 2A, the most upfield labeled diagonal resonance (at 1.52 ppm) shows a single cross peak to a proton in the Cα region at 4.40 ppm, suggesting an alanine residue (Ala-127), and indicating that the appropriate diagonal peak has an F_2 coordinate of 19.2 (and not 39.9) ppm. The adjacent diagonal resonance (originating from Ile-106) also shows a cross peak with an Hα resonance, but in addition, three more cross peaks to the two nonequivalent Cγ methylene protons and to the Cγ_m methyl protons are observed. This pattern of resonances is characteristic of an isoleucine residue, suggesting that the 39.9 (and not 19.2) ppm F_2 shift corresponds to the diagonal resonance. In the few cases where it may not be immediately obvious which of the three possible F_2 values applies, the slices in question are compared with those of the 3D NOESY-HMQC spectrum, which has been recorded with exactly twice the ^{13}C spectral width (and only eight scans per t_1, t_2), and for which no ambiguity is present.

The slices shown in Fig. 2 are asymmetric about the $F_1 = F_3$ diagonal, because both diagonal and cross peaks are labeled with the ^{13}C shift of the diagonal resonances. Thus, pairs of mirror image cross peaks appear in different slices. For example, Fig. 2A shows the correlation between Ile-106 Hβ (diagonal) and Ile-106 CγH$_3$ (cross peak). A slice taken at the ^{13}C shift of the Ile-106 Cγ methyl carbon (Fig. 2B) shows the correlation between Ile-106 CγH$_3$ (diagonal) and Hβ (cross peak). Figure 2B also shows the characteristic symmetric patterns observed for diagonal resonances of nonequivalent methylene protons, as seen for Asn-107 and Asn-66.

There are several diagonal resonances present in the slices shown in Fig. 2 for which no cross peaks appear. This is caused by the broader F_2 lineshape of the diagonal resonances relative to the cross peaks, as discussed above. For example, the diagonal resonance of Phe-42 Hα is clearly visible in Fig. 2B, whereas the cross peaks are absent in this slice. The adjacent slice, taken at $F_2 = 56.67$ ppm, shows intense cross peaks to the Hβ protons (data not shown).

The resonance intensity obtainable in a regular one-dimensional refocused INEPT ^{13}C spectrum is approximately equal for methine, methylene, and methyl carbons. This means that for methylene and methyl sites only one-half and approximately one-third of the ^{1}H magnetization can be transferred into net ^{13}C magnetization. Although a reverse INEPT transfers all ^{13}C magnetization back to the protons, for two nonequivalent methylene protons, each receives only one-half of the ^{13}C magnetization. The HCCH 3D technique employs a refocused INEPT transfer for magnetization transfer from protons to ^{13}C and a reverse refocused INEPT transfer from ^{13}C to protons. Therefore, correlations involving nonequivalent methylene protons are attenuated relative to magnetization transfer between vicinal methine protons. Thus, cross peaks between a methine and two nonequivalent methylene protons are attenuated twofold, and cross peaks between two pairs of nonequivalent methylene protons are attenuated fourfold. Correlations with methyl protons do not benefit from a threefold higher intensity, as observed in regular inverse detection experiments (*18*), but show the same intensity as cross peaks with methine protons. It is also easily calculated and confirmed experimentally that transfer via carbons with multiple ^{13}C neighbors (for example, Ile-Cβ) is attenuated relative to transfer via carbons that have only a single ^{13}C coupling partner (Ser, Asn, Asp, and Ala Cα–Cβ). Nevertheless, the spectra of Fig. 2 clearly indicate that the sensitivity obtainable in a 3 day experiment is sufficient to observe correlations between all types of vicinal protons.

The HCCH 3D spectrum provides nearly complete assignments of all aliphatic proton *and* ^{13}C resonances, with the exception of some resonances of the long aliphatic side chains (e.g., Lys, Arg) for which substantial overlap remains, even in the 3D spectrum. With virtually complete assignments of both ^{1}H and ^{13}C resonances in hand, it becomes quite straightforward to make a detailed analysis of a 3D NOESY-HMQC (*4, 5*) spectrum, providing the necessary information for protein structure determination.

ACKNOWLEDGMENTS

We thank Dr. Paul Wingfield for the sample of uniformly ^{15}N- and ^{13}C-labeled interleukin-1β. This work was supported by the Intramural AIDS Antiviral Program of the Office of the Director of the National

Institutes of Health (A.B., G.M.C., and A.M.G.). L.E.K. acknowledges financial support from the Medical Research Council of Canada and the Alberta Heritage Trust Foundation.

REFERENCES

1. D. MARION, L. E. KAY, S. W. SPARKS, AND D. A. TORCHIA, *J. Am. Chem. Soc.* **111,** 1515 (1989).
2. E. R. P. ZUIDERWEG AND S. W. FESIK, *Biochemistry* **28,** 2387 (1989).
3. D. MARION, P. C. DRISCOLL, L. E. KAY, P. T. WINGFIELD, A. BAX, A. M. GRONENBORN, AND G. M. CLORE, *Biochemistry* **28,** 6150 (1989).
4. M. IKURA, L. E. KAY, R. TSCHUDIN, AND A. BAX, *J. Magn. Reson.* **86,** 204 (1990).
5. E. R. P. ZUIDERWEG, L. P. MCINTOSH, F. W. DAHLQUIST, AND S. W. FESIK, *J. Magn. Reson.* **86,** 210 (1990).
6. S. W. FESIK, R. T. GAMPE, AND E. R. P. ZUIDERWEG, *J. Am. Chem. Soc.* **111,** 770 (1989).
7. S. S. WIJMENGA, K. HALLENGA, AND C. W. HILBERS, *J. Magn. Reson.* **84,** 634 (1989).
8. L. E. KAY, M. IKURA, AND A. BAX, *J. Am. Chem. Soc.* **112,** 888 (1990).
9. G. A. MORRIS AND R. FREEMAN, *J. Am. Chem. Soc.* **101,** 760 (1979).
10. D. P. BURUM AND R. R. ERNST, *J. Magn. Reson.* **39,** 163 (1980).
11. A. J. SHAKA, J. KEELER, AND R. FREEMAN, *J. Magn. Reson.* **53,** 313 (1983).
12. G. A. MORRIS AND R. FREEMAN, *J. Magn. Reson.* **29,** 433 (1978).
13. L. E. KAY, D. MARION, AND A. BAX, *J. Magn. Reson.* **84,** 72 (1989).
14. G. BODENHAUSEN, H. KOGLER, AND R. R. ERNST, *J. Magn. Reson.* **58,** 370 (1984).
15. M. H. LEVITT AND R. FREEMAN, *J. Magn. Reson.* **33,** 473 (1979).
16. M. IKURA, L. E. KAY, AND A. BAX, *Biochemistry,* submitted.
17. P. C. DRISCOLL, G. M. CLORE, D. MARION, P. WINGFIELD, AND A. M. GRONENBORN, *Biochemistry,* in press.
18. M. F. SUMMERS, L. G. MARZILLI, AND A. BAX, *J. Am. Chem. Soc.* **108,** 4285 (1986).
19. D. MARION, M. IKURA, R. TSCHUDIN, AND A. BAX, *J. Magn. Reson.* **85,** 393 (1989).